Numer. Math. Theor. Meth. Appl.
doi: 10.4208/nmtma.OA-2022-0004s

Vol. **15**, No. 4, pp. 990-1008
November 2022

A Dual-Horizon Nonlocal Diffusion Model and Its Finite Element Discretization

Mingchao Bi[1], Lili Ju[2] and Hao Tian[1,*]

[1] *School of Mathematical Sciences, Ocean University of China, Qingdao, Shandong 266100, China*
[2] *Department of Mathematics, University of South Carolina, Columbia, SC 29208, USA*

Received 3 December 2020; Accepted (in revised version) 8 October 2021

Abstract. In this paper, we present a dual-horizon nonlocal diffusion model, in which the influence area at each point consists of a standard sphere horizon and an irregular dual horizon and its geometry is determined by the distribution of the varying horizon parameter. We prove the mass conservation and maximum principle of the proposed nonlocal model, and establish its well-posedness and convergence to the classical diffusion model. Noticing that the dual horizon-related term in fact vanishes in the corresponding variational form of the model, we then propose a finite element discretization for its numerical solution, which avoids the difficulty of accurate calculations of integrals on irregular intersection regions between the mesh elements and the dual horizons. Various numerical experiments in two and three dimensions are also performed to illustrate the usage of the variable horizon and demonstrate the effectiveness of the numerical scheme.

AMS subject classifications: 65R20, 65N35, 74S05

Key words: Nonlocal diffusion, dual-horizon, maximum principle, finite element discretization, asymptotically compatible.

1. Introduction

In recent years, a number of nonlocal models in the form of integral-type formulations rather than partial differential equations have been developed, which allow them to reduce the regularity requirements and capture long-range interactions at different scales. Nonlocal continuum models can provide a more accurate description for a broad spectrum of applications from fracture mechanics [1, 24, 25, 28, 29, 33–36, 44], diffusion process [27, 32], image analysis [3, 21, 22], biology [30], phase transition [12, 15]

*Corresponding author. *Email addresses:* bmc@stu.ouc.edu.cn (M. Bi), ju@math.sc.edu (L. Ju), haot@ouc.edu.cn (H. Tian)

to mathematical analysis and computational simulations [2, 4–11, 13, 14, 16–20, 23, 26, 41–43, 45–47]. Among these, we are particularly interested in the nonlocal diffusion models taking the following form:

$$-\int_{\mathcal{B}(\boldsymbol{x},\delta)} \rho_\delta\big(\|\boldsymbol{y}-\boldsymbol{x}\|\big)\big(u(\boldsymbol{y})-u(\boldsymbol{x})\big)\,d\boldsymbol{y} = f(\mathbf{x}), \tag{1.1}$$

where u is the unknown function, f is the source function, $\mathcal{B}(\boldsymbol{x},\delta)$ is a neighborhood of $\mathbf{x}$, named as the horizon with δ denoting its sizing parameter, and $\rho_\delta(\|\boldsymbol{y}-\boldsymbol{x}\|)$ is a nonnegative symmetric weight function with $\|\cdot\|$ denoting the Euclidean metric. The horizon parameter δ has been usually treated as a constant until recently. Basically there are two major motivations to take a spatially variable horizon. The first is for the sake of computational efficiency, it is often necessary to vary the horizon sizes with respect to the spatial distribution of the material points, e.g. for adaptive refinement. In the implementation of traditional nonlocal diffusion models with constant horizon radius, the horizon has to be determined with respect to the lowest requirement of resolution in order to achieve acceptable accuracy [31]. The other is to allow the horizon parameter to vanish as the material points approach to the boundary, so that the traditional boundary condition could be directly imposed to the nonlocal diffusion models [37, 40].

In the past few years, some nonlocal models with variable horizons have been developed, including the dual-horizon peridynamics for nonlocal mechanics [31] and nonlocal diffusion models allowing heterogeneous localization [40]. In [31] the ideal of dual-horizon was firstly proposed in the area of peridynamics, which is derived based on the Newton's third law. In this model, the influence area for a point includes both a traditional sphere horizon and a dual-horizon, and the geometry of the dual-horizon can be highly irregular depending on the distribution of the horizon at each point. The dual-horizon peridynamics is discretized using the meshfree method in [31], and with such a discretization scheme, the quadratures on the intersection areas between the mesh elements and the horizons/the dual-horizons must be calculated. On the other hand, due to the high irregularity of these regions, these integrals on dual horizons are quite hard be calculated with high accuracy, especially for high dimensional problems. In [37, 40], nonlocal diffusion models with a shrinking horizon as it approaches the inner interface (where the nonlocal models and local models connect) are proposed, as well as the weak formulation of the nonlocal models with variable horizon. In addition, the finite element discretization is used for their numerical approximation and some numerical examples of one-dimension problems are presented.

In this paper, we propose a dual-horizon nonlocal diffusion model. The basic structure of our model is consistent with the dual-horizon peridynamics proposed in [31], in which the integral equation include two parts, one is with the traditional sphere horizon $B(\mathbf{x},\delta(\mathbf{x}))$ and the other is with an irregular dual horizon $\widetilde{B}(\mathbf{x},\delta(\mathbf{y}))$. We present rigorous mathematical analysis on the proposed nonlocal model and its numerical discretization. We prove the mass conservation, the maximum principle and the well-posedness of the model, in addition to the convergence to the local classic diffusion

equation as the nonlocal horizon parameter approaches to zero. On its numerical discretization, we focus on developing a finite element approximation, with which we only need deal with the integrals on the traditional sphere horizons. Such property is very important to develop effective numerical schemes for two and three dimensional problems. In addition, standard Galerkin continuous finite element methods are known to be asymptotically compatible [38, 39], i.e., the approximate solution always converges to the exact solution of the classical diffusion problem when the horizon parameter and the grid size go to zero simultaneously.

The rest of the paper is organized as follows: some notations are first introduced in Section 1.1, then the formulation of the dual-horizon nonlocal diffusion model and its mathematical analysis are presented in Section 2. Next we propose a finite element discretization for the proposed nonlocal model and discuss its implementation together with asymptotic compatibility in Section 3. Various numerical experiments in two and three dimensions are performed to validate the theoretical results. Finally, some concluding remarks are given in Section 5.

1.1. Notations

We use the following notations throughout the paper. Let Ω_s be an open, connected and bounded domain in $\mathbb{R}^n$. The horizon parameter $\delta > 0$ represents the maximum distance within which nonlocal interaction can happen, which could be a constant or spatially dependent. Let Ω_c be an interaction domain for the specification of volume constrained boundary conditions [8] and set $\Omega = \Omega_s \cup \Omega_c$. Let $\boldsymbol{\alpha}(\mathbf{x}, \mathbf{y}) : \mathbb{R}^n \times \mathbb{R}^n \to \mathbb{R}^n$ be a two-point vector mapping which is anti-symmetric, i.e., $\boldsymbol{\alpha}(\mathbf{y}, \mathbf{x}) + \boldsymbol{\alpha}(\mathbf{x}, \mathbf{y}) = 0$. In the theory of nonlocal vector calculus [8, 9], the action of the nonlocal divergence operator on a locally integrable two-point vector function $\boldsymbol{\nu}(\mathbf{x}, \mathbf{y})$, $\mathcal{D}(\boldsymbol{\nu}) : \mathbb{R}^n \to \mathbb{R}$, is defined as

$$\mathcal{D}(\boldsymbol{\nu})(\mathbf{x}) := \int_{\mathbb{R}^n} \big(\boldsymbol{\nu}(\mathbf{x}, \mathbf{y}) + \boldsymbol{\nu}(\mathbf{y}, \mathbf{x})\big)^T \cdot \boldsymbol{\alpha}(\mathbf{x}, \mathbf{y})\, d\mathbf{y} \quad \text{for} \quad \mathbf{x} \in \mathbb{R}^n. \tag{1.2}$$

For any scalar function $u : \mathbb{R}^n \to \mathbb{R}$, the adjoint operator $\mathcal{D}^*(u) : \mathbb{R}^n \times \mathbb{R}^n \to \mathbb{R}^n$ of the nonlocal divergence operator $\mathcal{D}$ is defined as

$$\mathcal{D}^*(u)(\mathbf{x}, \mathbf{y}) = \big(u(\mathbf{x}) - u(\mathbf{y})\big)\boldsymbol{\alpha}(\mathbf{x}, \mathbf{y}) \quad \text{for} \quad \mathbf{x}, \mathbf{y} \in \mathbb{R}^n. \tag{1.3}$$

Without loss of generality, we assume in this paper that

$$\boldsymbol{\alpha}(\mathbf{x}, \mathbf{y}) = \frac{\mathbf{y} - \mathbf{x}}{\|\mathbf{y} - \mathbf{x}\|} \quad \text{for} \quad \mathbf{x}, \mathbf{y} \in \mathbb{R}^n, \tag{1.4}$$

which is commonly used in peridynamics and many nonlocal models [8, 9, 14].

2. A dual-horizon nonlocal diffusion model and its properties

We first present our dual-horizon nonlocal diffusion model. Let the variable horizon parameter $\delta(\mathbf{x})$ be a Lipschitz continuous positive function defined over $\overline{\Omega}$ such that

$0 < \delta_{\min} \le \delta(\mathbf{x}) \le \delta_{\max}$. In this case, we take $\Omega_c = \{\mathbf{x} \in \mathbb{R}^n \setminus \Omega_s \,|\, \mathrm{dist}(\mathbf{x}, \Omega_s) \le \max_{\mathbf{y}\in\Omega_s} \delta(\mathbf{y})\}$. For any $\mathbf{x}, \mathbf{y} \in \mathbb{R}^n$, let us define a two-point indicator function as

$$1_{\delta(\mathbf{x})}(\mathbf{x}, \mathbf{y}) = \begin{cases} 1, & \text{if} \quad \|\mathbf{y} - \mathbf{x}\| < \delta(\mathbf{x}), \\ 0, & \text{otherwise}, \end{cases} \tag{2.1}$$

and a positive nonlocal influence function $\kappa(\mathbf{x}, \mathbf{y})$ satisfying $\kappa(\mathbf{x}, \mathbf{y}_1) = \kappa(\mathbf{x}, \mathbf{y}_2)$ for any $\|\mathbf{y}_1 - \mathbf{x}\| = \|\mathbf{y}_2 - \mathbf{x}\|$ and

$$\int_{B(\mathbf{0},\delta(\mathbf{x}))} z_i z_j \kappa(\mathbf{x}, \mathbf{x} + \mathbf{z})\, d\mathbf{z} = \delta_{ij}. \tag{2.2}$$

Note that the above integral is written in terms of the Cartesian coordinates and δ_{ij} here represents the Kronecker delta. An example of kernels satisfying (2.2) can be given by

$$\kappa(\mathbf{x}, \mathbf{y}) = \frac{n(n+2-s)}{\beta_n \delta(\mathbf{x})^{n+2-s}} \frac{1}{\|\mathbf{y} - \mathbf{x}\|^s}, \tag{2.3}$$

where

$$\beta_n = \frac{n\pi^{n/2}}{\Gamma(n/2+1)}$$

is the surface area of the unit sphere $B(\mathbf{0}, 1)$ in $\mathbb{R}^n$ and $0 \le s \le 2$ is a constant parameter that determines the kernel singularity of the nonlocal diffusion process. Then we define a diffusion weight function as

$$\omega(\mathbf{x}, \mathbf{y}) = 1_{\delta(\mathbf{x})}(\mathbf{x}, \mathbf{y}) \kappa(\mathbf{x}, \mathbf{y}). \tag{2.4}$$

Note that ω is used to measure the extent of influence of the nonlocal diffusion between two points $\mathbf{x}$ and $\mathbf{y}$ and not symmetric since

$$\omega(\mathbf{y}, \mathbf{x}) = 1_{\delta(\mathbf{y})}(\mathbf{y}, \mathbf{x}) \kappa(\mathbf{y}, \mathbf{x}) \ne \omega(\mathbf{x}, \mathbf{y}).$$

Given an isotropic diffusion coefficient tensor, i.e., a second order tensor $\boldsymbol{A}_{ij}(\mathbf{x}) = a(\mathbf{x})\boldsymbol{\delta}_{ij}$, where $\boldsymbol{\delta}_{ij}$ is the Kronecker delta function and $a \in L^\infty(\Omega)$ is a scalar function restricted with $0 < a_0 \le a(\mathbf{x}) \le a_1 < \infty$ for some positive constants a_0 and a_1, we define the corresponding two-point second-order tensor $\boldsymbol{\Theta} : \Omega \times \Omega \to \mathbb{R}$ for the nonlocal diffusion as

$$\boldsymbol{\Theta}(\mathbf{x}, \mathbf{y}) = \boldsymbol{A}(\mathbf{x}) \omega(\mathbf{x}, \mathbf{y}). \tag{2.5}$$

Finally, the nonlocal (isotropic) diffusion operator, $\mathcal{L}^{\mathrm{diff}}$ is constructed as

$$\mathcal{L}^{\mathrm{diff}} u(\mathbf{x}) = \mathcal{D}(\boldsymbol{\Theta} \cdot \mathcal{D}^* u)(\mathbf{x}) \quad \text{for} \quad \mathbf{x} \in \Omega_s. \tag{2.6}$$

We now summarize the new nonlocal diffusion model as follows:

$$\begin{cases} \mathcal{L} u = f, & \mathbf{x} \in \Omega_s, \\ u = g, & \mathbf{x} \in \Omega_c, \end{cases} \tag{2.7}$$

where $\mathcal{L}u = \mathcal{L}^{\text{diff}}u$, $f \in L^2(\Omega_s)$ and $g \in L^2(\Omega_c)$. The problem (2.7) is an integral equation in Ω_s along with a nonlocal volumetrically constrained Dirichlet boundary condition in the interaction domain Ω_c [8]. For more discussions on nonlocal boundary conditions, we refer to [8] for a general set-up and [17] and references cited therein for additional studies on Neumann (traction) boundary conditions.

By substituting $\mathcal{L}$ in (2.7) with (2.6) and noticing that

$$\boldsymbol{\alpha}(\mathbf{x},\mathbf{y})^T \cdot \boldsymbol{A}(\mathbf{x}) \cdot \boldsymbol{\alpha}(\mathbf{x},\mathbf{y}) = a(\mathbf{x}),$$

we obtain the formulation of the nonlocal diffusion equation as: for any $\mathbf{x} \in \Omega_s$,

$$\int_\Omega \big(\boldsymbol{A}(\mathbf{x}) \cdot \boldsymbol{\alpha}(\mathbf{x},\mathbf{y})\omega(\mathbf{x},\mathbf{y})(u(\mathbf{x}) - u(\mathbf{y})) + \boldsymbol{A}(\mathbf{y}) \cdot \boldsymbol{\alpha}(\mathbf{y},\mathbf{x})\omega(\mathbf{y},\mathbf{x})(u(\mathbf{y}) - u(\mathbf{x}))\big)^T \cdot \boldsymbol{\alpha}(\mathbf{x},\mathbf{y})\, d\mathbf{y} = f(\mathbf{x}),$$

or equivalently,

$$-\int_\Omega a(\mathbf{x})\omega(\mathbf{x},\mathbf{y})\big(u(\mathbf{y}) - u(\mathbf{x})\big)d\mathbf{y} - \int_\Omega a(\mathbf{y})\omega(\mathbf{y},\mathbf{x})\big(u(\mathbf{y}) - u(\mathbf{x})\big)d\mathbf{y} = f(\mathbf{x}). \quad (2.8)$$

We also remark that the corresponding local diffusion model is given by

$$\begin{cases} -\nabla \cdot (a\nabla u) = f, & \mathbf{x} \in \Omega, \\ u = g, & \mathbf{x} \in \partial\Omega. \end{cases} \quad (2.9)$$

Let us take a careful look at the influence regions of the two-point indicator functions $1_{\delta(\mathbf{x})}(\mathbf{x},\mathbf{y})$ (see its definition in (2.1)). For any given subdomain $U \in \Omega$, we denote its characteristic function as 1_U such that

$$\begin{cases} 1_U(\mathbf{x}) = 1, & \text{if} \quad \mathbf{x} \in U, \\ 1_U(\mathbf{x}) = 0, & \text{otherwise.} \end{cases}$$

For the nonlocal diffusion operator, the influence region of $1_{\delta(\mathbf{x})}(\mathbf{x},\mathbf{y})$ for a fixed point $\mathbf{x} \in \Omega_s$ is the sphere $B(\mathbf{x},\delta(\mathbf{x}))$ (see the left picture of Fig. 1). We then have $1_{\delta(\mathbf{x})}(\mathbf{x},\mathbf{y}) = 1_{B(\mathbf{x},\delta(\mathbf{x}))}(\mathbf{y})$ for any $\mathbf{x},\mathbf{y} \in \Omega$. For the second integral in (2.8), the corresponding indicator function can be expressed as

$$1_{\delta(\mathbf{y})}(\mathbf{y},\mathbf{x}) = \begin{cases} 1, & \text{if} \quad \|\mathbf{y} - \mathbf{x}\| < \delta(\mathbf{y}), \\ 0, & \text{otherwise.} \end{cases} \quad (2.10)$$

Let we denote by $\widetilde{B}(\mathbf{x},\delta(\mathbf{y}))$ the influence region of $1_{\delta(\mathbf{y})}(\mathbf{y},\mathbf{x})$ for a fixed point $\mathbf{x}$ (see the right picture of Fig. 1), i.e., $1_{\delta(y)}(\mathbf{y},\mathbf{x}) = 1_{\widetilde{B}(\mathbf{x},\delta(\mathbf{y}))}(\mathbf{y})$. Thus, (2.8) can be further transformed into

$$-\int_{B(\mathbf{x},\delta(\mathbf{x}))} a(\mathbf{x})\kappa(\mathbf{x},\mathbf{y})\big(u(\mathbf{y}) - u(\mathbf{x})\big)d\mathbf{y} - \int_{\widetilde{B}(\mathbf{x},\delta(\mathbf{y}))} a(\mathbf{y})\kappa(\mathbf{y},\mathbf{x})\big(u(\mathbf{y}) - u(\mathbf{x})\big)d\mathbf{y} = f(\mathbf{x}). \quad (2.11)$$

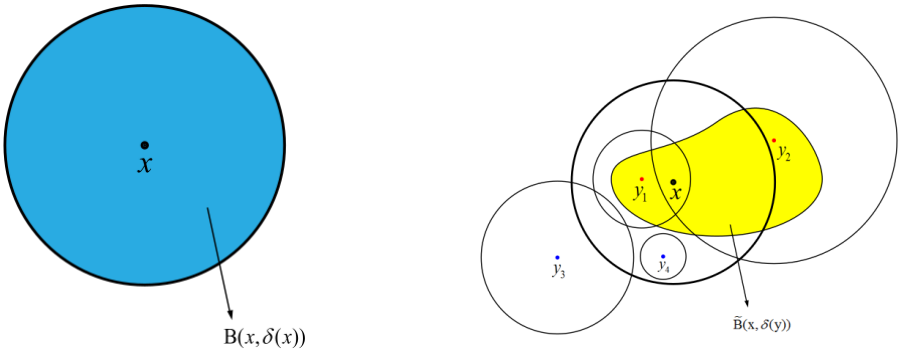

Figure 1: Illustration of the influence regions of the indicator functions for the dual-horizon nonlocal diffusion model (2.7). Left: the horizon $B(\mathbf{x},\delta(\mathbf{x}))$; right: the dual horizon $\widetilde{B}(\mathbf{x},\delta(\mathbf{y}))$. For the points $\mathbf{y}_1$ and $\mathbf{y}_2$, their influence areas $B(\mathbf{y}_1,\delta(\mathbf{y}_1))$ and $B(\mathbf{y}_2,\delta(\mathbf{y}_2))$ include the point $\mathbf{x}$, thus $\mathbf{y}_1$ and $\mathbf{y}_2$ belong to $\widetilde{B}(\mathbf{x},\delta(\mathbf{y}))$. Meanwhile, for the points $\mathbf{y}_3$ and $\mathbf{y}_4$, their influence areas $B(\mathbf{y}_3,\delta(\mathbf{y}_3))$ and $B(\mathbf{y}_4,\delta(\mathbf{y}_4))$ do not include the point $\mathbf{x}$, thus $\mathbf{y}_3$ and $\mathbf{y}_4$ do not belong to $\widetilde{B}(\mathbf{x},\delta(\mathbf{y}))$.

Note that $\widetilde{B}(\mathbf{x},\delta(\mathbf{y}))$ is defined as a union of points $\mathbf{y}$ whose horizons $B(\mathbf{y},\delta(\mathbf{y}))$ include $\mathbf{x}$. Thus the shape of $\widetilde{B}(\mathbf{x},\delta(\mathbf{y}))$ would be determined by the distribution of $\delta(\mathbf{y})$, thus could be highly irregular.

Remark 2.1. If we take the horizon function to be constant $\delta(\mathbf{x})\equiv\delta$, the dual horizon $\widetilde{B}(\mathbf{x},\delta(\mathbf{y}))$ would become the standard sphere horizon $B(\mathbf{x},\delta)$, and Eq. (2.11) then degenerate into a traditional nonlocal diffusion model with constant horizon

$$-\int_{B(\mathbf{x},\delta)}\big(a(\mathbf{x})+a(\mathbf{y})\big)\kappa(\mathbf{x},\mathbf{y})\big(u(\mathbf{y})-u(\mathbf{x})\big)d\mathbf{y}=f(\mathbf{x}). \tag{2.12}$$

2.1. Mass conservation and maximum principle

For any point $\mathbf{y}\in\widetilde{B}(\mathbf{x},\delta(\mathbf{y}))$, the bond $\mathbf{xy}$ is actually the bond $\mathbf{yx}$ in $B(\mathbf{y},\delta(\mathbf{y}))$. The bond $\mathbf{xy}$ exerts action from $\mathbf{y}$ to $\mathbf{x}$ and the bond $\mathbf{yx}$ is the reaction from $\mathbf{y}$ to $\mathbf{x}$, thus the mass conservation can be guaranteed by the dual-horizon nonlocal diffusion model (2.7) as shown below.

Let us define

$$\boldsymbol{\gamma}(\mathbf{x},\mathbf{y})=a(\mathbf{x})\omega(\mathbf{x},\mathbf{y})+a(\mathbf{y})\omega(\mathbf{y},\mathbf{x}), \tag{2.13}$$

which can be regarded as a symmetric kernel function for the whole nonlocal diffusion operator. We have $\boldsymbol{\gamma}(\mathbf{x},\mathbf{y})\geq 0$ for any $\mathbf{x},\mathbf{y}\in\Omega$. It is easy to verify that the diffusion nonlocal operator $\mathcal{L}$ can be rewritten as

$$\mathcal{L}u(\mathbf{x})=\int_{\Omega}\big(u(\mathbf{x})-u(\mathbf{y})\big)\boldsymbol{\gamma}(\mathbf{x},\mathbf{y})d\mathbf{y}. \tag{2.14}$$

By integrating both sides of (2.14) on Ω_s, we then have

$$\int_{\Omega_s}\mathcal{L}u(\mathbf{x})d\mathbf{x}=\int_{\Omega_s}\int_{\Omega_c\cup\Omega_s}\big(u(\mathbf{x})-u(\mathbf{y})\big)\boldsymbol{\gamma}(\mathbf{x},\mathbf{y})\,d\mathbf{y}d\mathbf{x}$$

$$= \int_{\Omega_s}\int_{\Omega_c} \big(u(\mathbf{x}) - u(\mathbf{y})\big)\boldsymbol{\gamma}(\mathbf{x},\mathbf{y})\, d\mathbf{y}d\mathbf{x} + \int_{\Omega_s}\int_{\Omega_s} \big(u(\mathbf{x}) - u(\mathbf{y})\big)\boldsymbol{\gamma}(\mathbf{x},\mathbf{y})\, d\mathbf{y}d\mathbf{x}.$$

By interchanging the variable $\mathbf{x}$ and $\mathbf{y}$, we have

$$\begin{aligned}
&\int_{\Omega_s}\int_{\Omega_s} \big(u(\mathbf{x}) - u(\mathbf{y})\big)\boldsymbol{\gamma}(\mathbf{x},\mathbf{y})\, d\mathbf{y}d\mathbf{x} \\
&= \frac{1}{2}\int_{\Omega_s}\int_{\Omega_s} \Big(\big(u(\mathbf{x}) - u(\mathbf{y})\big)\boldsymbol{\gamma}(\mathbf{x},\mathbf{y}) + \big(u(\mathbf{y}) - u(\mathbf{x})\big)\boldsymbol{\gamma}(\mathbf{y},\mathbf{x})\Big) d\mathbf{y}d\mathbf{x} \\
&= \frac{1}{2}\int_{\Omega_s}\int_{\Omega_s} \Big(\big(u(\mathbf{x}) - u(\mathbf{y})\big)\boldsymbol{\gamma}(\mathbf{x},\mathbf{y}) + \big(u(\mathbf{y}) - u(\mathbf{x})\big)\boldsymbol{\gamma}(\mathbf{x},\mathbf{y})\Big) d\mathbf{y}d\mathbf{x} = 0,
\end{aligned}$$

which means the flux from Ω_s into itself is zero, i.e., there are no net self-interactions [9]. Thus it holds that

$$\int_{\Omega_s} \mathcal{L}u(\mathbf{x})d\mathbf{x} = \int_{\Omega_s}\int_{\Omega_c} \big(u(\mathbf{x}) - u(\mathbf{y})\big)\boldsymbol{\gamma}(\mathbf{x},\mathbf{y})\, d\mathbf{y}d\mathbf{x}, \tag{2.15}$$

and we obtain the mass conservation of the proposed nonlocal model as

$$\int_{\Omega_s}\int_{\Omega_c} \big(u(\mathbf{x}) - u(\mathbf{y})\big)\boldsymbol{\gamma}(\mathbf{x},\mathbf{y})\, d\mathbf{y}d\mathbf{x} = \int_{\Omega_s} f(\mathbf{x})\, d\mathbf{x}. \tag{2.16}$$

Here, the left side term is the nonlocal flux from the interior domain Ω_s to the interaction domain Ω_c while the right side term is the source from Ω_s, and putting together they cancel out each other.

Theorem 2.1 (Maximum principle)**.** *Suppose that $\mathcal{L}u$ is well-defined in Ω_s. If $\mathcal{L}u < 0$ in Ω_s, then the nonnegative maximum of u must be attained in the interaction domain Ω_c.*

Proof. We will show that the nonnegative maximum can not be attained in Ω_s by contradiction. Assume that u attains a nonnegative maximum at $\mathbf{x}_0 \in \Omega_s$, i.e., $u(\mathbf{x}_0) = \max_{\mathbf{x}\in\Omega} u(\mathbf{x}) \geq 0$. By (2.8), we have

$$\begin{aligned}
\mathcal{L}u(\mathbf{x}_0) = &- \int_{B(\mathbf{x}_0,\delta(\mathbf{x}_0))} a(\mathbf{x}_0)\big(u(\mathbf{y}) - u(\mathbf{x}_0)\big)\kappa(\mathbf{x}_0,\mathbf{y})\, d\mathbf{y} \\
&- \int_{\widetilde{B}(\mathbf{x}_0,\delta(\mathbf{y}))} a(\mathbf{y})\big(u(\mathbf{y}) - u(\mathbf{x}_0)\big)\kappa(\mathbf{y},\mathbf{x}_0)\, d\mathbf{y}.
\end{aligned} \tag{2.17}$$

Since $u(\mathbf{y}) - u(\mathbf{x}_0) \leq 0$, it is easy to verify that the first integral in (2.17) satisfies

$$-\int_{B(\mathbf{x}_0,\delta(\mathbf{x}_0))} \overbrace{\big(a(\mathbf{x}_0)\big)}^{>0}\overbrace{\big(u(\mathbf{y}) - u(\mathbf{x}_0)\big)}^{\leq 0}\overbrace{\kappa(\mathbf{x}_0,\mathbf{y})}^{\geq 0}\, d\mathbf{y} \geq 0.$$

The second integral of (2.17) gives us

$$-\int_{\widetilde{B}(\mathbf{x},\delta(\mathbf{y}))} \overbrace{\big(a(\mathbf{y})\big)}^{>0}\overbrace{\big(u(\mathbf{y}) - u(\mathbf{x}_0)\big)}^{\leq 0}\overbrace{\kappa(\mathbf{y},\mathbf{x}_0)}^{\geq 0}\, d\mathbf{y} \geq 0.$$

Hence, we get $\mathcal{L}u(\mathbf{x}_0) \geq 0$, which contradicts the assumption $\mathcal{L}u(\mathbf{x}_0) < 0$. □

2.2. Weak formulation and well-posedness

Eq. (2.8) can be regarded as the strong form of our nonlocal diffusion model. Without loss of generality, we next consider the case of homogeneous nonlocal boundary condition $g(\mathbf{x}) = 0$ for $\mathbf{x} \in \Omega_c$ and $f \in L^2(\Omega_s)$. Let us define the constrained space $L^2_{n0}(\Omega) = \{u \in L^2(\Omega) : u|_{\Omega_c} = 0\}$ and denote by $(\cdot,\cdot)$ the resulted L^2 inner product. Then a weak formulation of the nonlocal diffusion problem (2.8) is: find $u \in L^2_{n0}(\Omega)$ such that

$$\mathbf{B}(u,v) = \mathbf{F}(v), \quad \forall v \in L^2_{n0}(\Omega), \tag{2.18}$$

where the bilinear functional $\mathbf{B}(u,v) = (\mathcal{L}u, v)$, i.e.,

$$\begin{aligned}\mathbf{B}(u,v) &= \int_\Omega \int_\Omega \big(u(\mathbf{x}) - u(\mathbf{y})\big)\boldsymbol{\gamma}(\mathbf{x},\mathbf{y})v(\mathbf{x})\, d\mathbf{y}d\mathbf{x} \\ &= \frac{1}{2}\int_\Omega \int_\Omega \boldsymbol{\gamma}(\mathbf{x},\mathbf{y})\big(u(\mathbf{x}) - u(\mathbf{y})\big)\big(v(\mathbf{x}) - v(\mathbf{y})\big)\, d\mathbf{y}d\mathbf{x},\end{aligned} \tag{2.19}$$

which is consistent with the form discussed in [37], and the linear functional $\mathbf{F}(v) = (f,v)$. Let us consider the weight functions w defined in (2.4), it is determined by κ given in (2.3) with $0 \le s \le 2$. Furthermore, with $0 < \delta_{\min} \le \delta(\mathbf{x}) \le \delta_{\max}$ and $0 < a_0 \le a(\mathbf{x}) \le a_1 < \infty$, it is not hard to find that the kernel γ satisfies

$$\int_\Omega \boldsymbol{\gamma}(\mathbf{x},\mathbf{y})\, d\mathbf{y} \le K_1, \quad \int_{\Omega_c} \boldsymbol{\gamma}(\mathbf{y},\mathbf{x}) d\mathbf{y} \ge K_2, \quad \forall \mathbf{x} \in \Omega \tag{2.20}$$

for some positive constants $K_1 > 0$ and $K_2 > 0$, which depends on $\delta_{\min}$, $\delta_{\max}$, a_0 and a_1. Under these conditions, the nonlocal operator $\mathcal{L}$ is bounded in $L^2_{n0}(\Omega)$ so that a weak solution is also a strong solution of (2.8) in $L^2_{n0}(\Omega)$.

Theorem 2.2 (Well-posedness)**.** *There exists a unique solution $u \in L^2_{n0}(\Omega)$ to the nonlocal diffusion problem* (2.8)*. Furthermore, the solution satisfies the a priori estimate*

$$\|u\|_{L^2(\Omega)} \le \frac{2}{K_2}\|f\|_{L^2(\Omega)}. \tag{2.21}$$

Proof. First, it is easy to see that

$$|\mathbf{F}(v)| \le \|f\|_{L^2(\Omega)}\|v\|_{L^2(\Omega_s)}. \tag{2.22}$$

We now show that the bilinear operator $\mathbf{B}(\cdot,\cdot)$ is bounded on $L^2_{n0}(\Omega) \times L^2_{n0}(\Omega)$. It holds that for any $u, v \in L^2_{n0}(\Omega)$,

$$\begin{aligned}\mathbf{B}(u,v) &= \int_\Omega \int_\Omega \big(u(\mathbf{x}) - u(\mathbf{y})\big)\boldsymbol{\gamma}(\mathbf{x},\mathbf{y})v(\mathbf{x})\, d\mathbf{y}d\mathbf{x} \\ &= \int_\Omega \int_\Omega u(\mathbf{x})v(\mathbf{x})\boldsymbol{\gamma}(\mathbf{x},\mathbf{y})\, d\mathbf{y}d\mathbf{x} - \int_\Omega \int_\Omega u(\mathbf{x})v(\mathbf{y})\boldsymbol{\gamma}(\mathbf{x},\mathbf{y})\, d\mathbf{y}d\mathbf{x}.\end{aligned} \tag{2.23}$$

Using the first inequality in (2.20), we have that

$$\begin{aligned}&\left|\int_\Omega\int_\Omega u(\mathbf{x})v(\mathbf{x})\boldsymbol{\gamma}(\mathbf{x},\mathbf{y})\ d\mathbf{y}d\mathbf{x}\right|\\&=\left|\int_\Omega u(\mathbf{x})v(\mathbf{x})\int_\Omega\boldsymbol{\gamma}(\mathbf{x},\mathbf{y})\ d\mathbf{y}d\mathbf{x}\right|\le K_1\|u\|_{L^2(\Omega)}\|v\|_{L^2(\Omega)}\end{aligned}$$

and

$$\begin{aligned}&\left|\int_\Omega\int_\Omega\big(u(\mathbf{x})v(\mathbf{y})\boldsymbol{\gamma}(\mathbf{x},\mathbf{y})\big)\,d\mathbf{y}d\mathbf{x}\right|\\&\le\left(\int_\Omega\int_\Omega u^2(\mathbf{x})\boldsymbol{\gamma}(\mathbf{x},\mathbf{y})d\mathbf{y}d\mathbf{x}\right)^{\frac12}\left(\int_\Omega\int_\Omega v(\mathbf{y})^2\boldsymbol{\gamma}(\mathbf{x},\mathbf{y})\,d\mathbf{y}d\mathbf{x}\right)^{\frac12}\\&=\left(\int_\Omega u^2(\mathbf{x})\int_\Omega\boldsymbol{\gamma}(\mathbf{x},\mathbf{y})\,d\mathbf{y}d\mathbf{x}\right)^{\frac12}\left(\int_\Omega v(\mathbf{x})^2\int_\Omega\boldsymbol{\gamma}(\mathbf{y},\mathbf{x})\ d\mathbf{y}d\mathbf{x}\right)^{\frac12}\\&\le K_1\|u\|_{L^2(\Omega)}\|v\|_{L^2(\Omega)},\end{aligned}$$

thus

$$|\mathbf{B}(u,v)|\le 2K_1\|u\|_{L^2(\Omega)}\|v\|_{L^2(\Omega)}.$$

Next we show that the bilinear operator $B(\cdot,\cdot)$ is coercive on $L^2_{n0}(\Omega)$. Note that

$$\begin{aligned}\mathbf{B}(u,u)&=\frac12\int_\Omega\int_\Omega\big(u(\mathbf{y})-u(\mathbf{x})\big)^2\gamma(\mathbf{y},\mathbf{x})d\mathbf{y}d\mathbf{x}\\&\ge\frac12\int_\Omega\int_{\Omega_c}\big(u(\mathbf{y})-u(\mathbf{x})\big)^2\gamma(\mathbf{y},\mathbf{x})d\mathbf{y}d\mathbf{x}\\&=\frac12\int_\Omega u(\mathbf{x})^2\int_{\Omega_c}\gamma(\mathbf{y},\mathbf{x})dyd\mathbf{x}\\&\ge\frac12\int_\Omega u(\mathbf{x})^2K_2d\mathbf{x}=\frac{K_2}{2}\|u\|^2_{L^2(\Omega)}.\end{aligned}\tag{2.24}$$

By the Lax-Milgram theorem, there exists a unique weak (and thus strong) solution $u\in L^2_{n0}(\Omega)$ to the problem (2.18). Finally, because

$$\frac{K_2}{2}\|u\|^2_{L^2(\Omega)}\le\boldsymbol{B}(u,u)=|\mathbf{F}(u)|\le\|f\|_{L^2(\Omega)}\|u\|_{L^2(\Omega)},$$

we have the a priori estimate (2.21). □

2.3. Local limit

Next we analyze the local limit of the nonlocal weak formulation (2.18) as the horizon $\delta(\mathbf{x})$ goes to zero.

Theorem 2.3 (Local limit). *If $u, v \in L^2_{n0}(\Omega) \cap C^2(\overline{\Omega})$, then*

$$\lim_{\delta_{\max}\to 0} \mathbf{B}(u,v) = (a\nabla u, \nabla v). \tag{2.25}$$

Proof. Note that

$$\begin{aligned}
\mathbf{B}(u,v) &= \int_\Omega \int_\Omega \big(u(\mathbf{x}) - u(\mathbf{y})\big)\boldsymbol{\gamma}(\mathbf{x},\mathbf{y})v(\mathbf{x})\, d\mathbf{y}d\mathbf{x} \\
&= \frac{1}{2}\int_\Omega \int_\Omega \boldsymbol{\gamma}(\mathbf{x},\mathbf{y})\big(u(\mathbf{y}) - u(\mathbf{x})\big)\big(v(\mathbf{y}) - v(\mathbf{x})\big)\, d\mathbf{y}d\mathbf{x} \\
&= \frac{1}{2}\int_\Omega \int_\Omega \big(a(\mathbf{x})\omega(\mathbf{x},\mathbf{y}) + a(\mathbf{y})\omega(\mathbf{y},\mathbf{x})\big) \\
&\quad \times \big(u(\mathbf{y}) - u(\mathbf{x})\big)\big(v(\mathbf{y}) - v(\mathbf{x})\big)\, d\mathbf{y}d\mathbf{x} \\
&= \int_\Omega \int_\Omega a(\mathbf{x})\omega(\mathbf{x},\mathbf{y})\big(u(\mathbf{y}) - u(\mathbf{x})\big)\big(v(\mathbf{y}) - v(\mathbf{x})\big) d\mathbf{y}d\mathbf{x}.
\end{aligned} \tag{2.26}$$

By using Taylor's expansion of u at $\mathbf{x}$ and interchanging the variables $\mathbf{x}$ and $\mathbf{y}$, the nonlocal bilinear form then can be written as

$$\begin{aligned}
\boldsymbol{B}(u,v) &= \int_\Omega a(\mathbf{x}) \int_\Omega \big(u(\mathbf{y}) - u(\mathbf{x})\big)\big(v(\mathbf{y}) - v(\mathbf{x})\big)\omega(\mathbf{x},\mathbf{y})\, d\mathbf{y}d\mathbf{x} \\
&= \int_\Omega a(\mathbf{x}) \int_{B(\mathbf{0},\delta(\mathbf{x}))} \Big(\nabla u(\mathbf{x})^T \mathbf{z}\mathbf{z}^T \nabla v(\mathbf{x}) + o\big(\|\mathbf{z}\|^2\big)\Big)\kappa(\mathbf{x},\mathbf{x}+\mathbf{z})\, d\mathbf{z}d\mathbf{x}.
\end{aligned} \tag{2.27}$$

According to (2.2) and (2.27), we obtain by simple calculations that

$$\lim_{\delta_{\max}\to 0} \boldsymbol{B}(u,v) = \lim_{\delta_{\max}\to 0} \left(\int_\Omega a(\mathbf{x})\nabla u(\mathbf{x})^T \nabla v(\mathbf{x})\, d\mathbf{x} + o(1)\right) = (a\nabla u, \nabla v),$$

which completes the proof. □

Note that the right-hand side of (2.25) is exactly the bilinear operator associated with the classic diffusion problem (2.9) with the boundary condition $g = 0$.

3. A finite element discretization and its implementation

In this section we propose a finite element scheme for discretizing the nonlocal diffusion problem (2.7). Let us first take another look at the bilinear functional (2.19)

$$\begin{aligned}
\mathbf{B}(u,v) &= \int_\Omega \int_\Omega \big(u(\mathbf{x}) - u(\mathbf{y})\big)\boldsymbol{\gamma}(\mathbf{x},\mathbf{y})v(\mathbf{x})\, d\mathbf{y}d\mathbf{x} \\
&= \int_\Omega \int_\Omega \big(u(\mathbf{x}) - u(\mathbf{y})\big)\big(a(\mathbf{x})\omega(\mathbf{x},\mathbf{y}) + a(\mathbf{y})\omega(\mathbf{y},\mathbf{x})\big)v(\mathbf{x})\, d\mathbf{y}d\mathbf{x} \\
&= \int_\Omega \int_\Omega \big(u(\mathbf{x}) - u(\mathbf{y})\big)a(\mathbf{x})\omega(\mathbf{x},\mathbf{y})v(\mathbf{x})\, d\mathbf{y}d\mathbf{x}
\end{aligned}$$

$$
\begin{aligned}
&+\int_\Omega\int_\Omega \big(u(\mathbf{x})-u(\mathbf{y})\big)a(\mathbf{y})\omega(\mathbf{y},\mathbf{x})v(\mathbf{x})\,d\mathbf{y}d\mathbf{x}\\
&=\int_\Omega\int_\Omega a(\mathbf{x})\omega(\mathbf{x},\mathbf{y})\big(u(\mathbf{x})-u(\mathbf{y})\big)\big(v(\mathbf{x})-v(\mathbf{y})\big)\,d\mathbf{y}d\mathbf{x}\\
&=\int_\Omega\int_{B(\mathbf{x},\delta(\mathbf{x}))} a(\mathbf{x})\kappa(\mathbf{x},\mathbf{y})\big(u(\mathbf{x})-u(\mathbf{y})\big)\big(v(\mathbf{x})-v(\mathbf{y})\big)\,d\mathbf{y}d\mathbf{x}. \qquad (3.1)
\end{aligned}
$$

Then we define the energy space as

$$
\mathcal{S}_\delta=\left\{u\in L^2(\Omega):\int_\Omega\int_{B(\mathbf{x},\delta(\mathbf{x}))} a(\mathbf{x})\kappa(\mathbf{x},\mathbf{y})\big(u(\mathbf{x})-u(\mathbf{y})\big)^2\,d\mathbf{y}d\mathbf{x}<\infty, u|_{\Omega_c}=0\right\},
$$

and clearly $\mathcal{S}_\delta$ is a subspace of $L^2(\Omega)$. Notice that in the above weak form only the integral over the sphere horizon $B(\mathbf{x},\delta(\mathbf{x}))$ is included, and the integral over the dual horizon $\widetilde{B}(\mathbf{x},\delta(\mathbf{y}))$ does not exist anymore. To distinguish the two representations of the equivalent bilinear functional, we denote the new one as

$$
(u,v)_{\mathcal{S}_\delta}=\int_\Omega\int_{B(\mathbf{x},_\delta(\mathbf{x}))} a(\mathbf{x})\kappa(\mathbf{x},\mathbf{y})\big(u(\mathbf{x})-u(\mathbf{y})\big)\big(v(\mathbf{x})-v(\mathbf{y})\big)\,d\mathbf{y}d\mathbf{x}, \qquad (3.2)
$$

and $\|\cdot\|_{\mathcal{S}_\delta}$ the associated norm as

$$
\|u\|_{\mathcal{S}_\delta}=\left\{\int_\Omega\int_{B(\mathbf{x},\delta(\mathbf{x}))} a(\mathbf{x})\kappa(\mathbf{x},\mathbf{y})\big(u(\mathbf{x})-u(\mathbf{y})\big)^2\,d\mathbf{x}d\mathbf{y}\right\}^{\frac{1}{2}}. \qquad (3.3)
$$

It can be shown that $\mathcal{S}_\delta$ is also the completion of $C_0^\infty(\Omega)$ in $L^2(\Omega_\delta)$ under the norm $\|\cdot\|_{s_\delta}$. Then the new weak formulations of (2.11) is as follows: find $u_\delta\in\mathcal{S}_\delta$ such that

$$
(u_\delta,v)_{\mathcal{S}_\delta}=(f,v)_{L^2},\quad \forall v\in\mathcal{S}_\delta. \qquad (3.4)
$$

Let us introduce the finite element space $V_{\delta,h}\subset\mathcal{S}_\delta$ associated with the mesh $\mathcal{T}_h=\{K\}$ of the domain Ω. We set

$$
V_{\delta,h}:=\big\{v\in\mathcal{S}_\delta: v|_K\in P(K),\forall K\in\mathcal{T}_h\big\},
$$

where $P(K)$ is the space of piecewise continuous polynomials on $\mathcal{T}_h$ with degree less than or equal to p ($p\geq 1$). As $h\to 0,\{V_{\delta,h}\}$ is dense in $\mathcal{S}_\delta$, i.e., for any $v\in\mathcal{S}_\delta$, there exists a sequence $(v_h\in V_{\delta,h})$ such that

$$
\|v_h-v\|_{\mathcal{S}_\delta}\to 0\quad\text{as}\quad h\to 0.
$$

These properties are easily satisfied by the standard finite element spaces. The Galerkin approximation in finite element method is then to replace $\mathcal{S}_\delta$ by $V_{\delta,h}$ in (3.4): find $u_{\delta,h}\in V_{\delta,h}$ such that

$$
(u_{\delta,h},v)_{S_\delta}=(f,v)_{L^2},\quad \forall v\in V_{\delta,h}. \qquad (3.5)
$$

Let $\{\phi_i\}$ be the set of basis functions of $V_{\delta,h}$ associated with the mesh nodes $\{\mathbf{x}_i\}_{i=1}^{N_s} \subset \Omega_s$, then the resulting linear system from the finite element discretization (3.5) can be expressed as follows:

$$A_h \vec{u}_h = \vec{f}, \tag{3.6}$$

where the unknown vector $\vec{u}_h = (u_h(\mathbf{x}_1), \cdots, u_h(\mathbf{x}_{N_s}))^T$, the coefficient matrix $A_h = (a_{i,j})_{1:N_s,1:N_s}$ with

$$a(i,j) = \int_\Omega \int_{B(\mathbf{x},\delta(\mathbf{x}))} a(\mathbf{x})\kappa(\mathbf{x},\mathbf{y})\big(\phi_i(\mathbf{y}) - \phi_i(\mathbf{x})\big)\big(\phi_j(\mathbf{y}) - \phi_j(\mathbf{x})\big)\, d\mathbf{y}d\mathbf{x}, \tag{3.7}$$

and the right-hand side $\vec{f} = (f(\mathbf{x}_1), \cdots, f(\mathbf{x}_{N_s}))^T$. The convergence of the above Galerkin continuous finite element discretization under the $\|\cdot\|_{\mathcal{S}_\delta}$ norm directly comes from the standard finite element theorem. Furthermore, such discretization is also known to be asymptotically compatible as analyzed in the framework of [37–39].

We can further divide the expression (3.7) into four integrals

$$\begin{aligned}
a_{i,j} &= \int_\Omega \int_{B(\mathbf{x},\delta(\mathbf{x}))} a(\mathbf{x})\kappa(\mathbf{x},\mathbf{y})\big(\phi_i(\mathbf{y}) - \phi_i(\mathbf{x})\big)\big(\phi_j(\mathbf{y}) - \phi_j(\mathbf{x})\big)\, d\mathbf{y}d\mathbf{x} \\
&= \int_{\Omega_s} a(\mathbf{x}) \int_{B(\mathbf{x},\delta(\mathbf{x}))} \kappa(\mathbf{x},\mathbf{y})\phi_i(\mathbf{y})\phi_j(\mathbf{y})\, d\mathbf{y}d\mathbf{x} \\
&\quad - \int_{\Omega_s} a(\mathbf{x})\phi_j(\mathbf{x}) \int_{B(\mathbf{x},\delta(\mathbf{x}))} \kappa(\mathbf{x},\mathbf{y})\phi_i(\mathbf{y})\, d\mathbf{y}d\mathbf{x} \\
&\quad - \int_{\Omega_s} a(\mathbf{x})\phi_i(\mathbf{x}) \int_{B(\mathbf{x},\delta(\mathbf{x}))} \kappa(\mathbf{x},\mathbf{y})\phi_j(\mathbf{y})\, d\mathbf{y}d\mathbf{x} \\
&\quad + \int_{\Omega_s} a(\mathbf{x})\phi_i(\mathbf{x})\phi_j(\mathbf{x}) \int_{B(\mathbf{x},\delta(\mathbf{x}))} \kappa(\mathbf{x},\mathbf{y})\, d\mathbf{y}d\mathbf{x} \\
&=: I_1 - I_2 - I_3 + I_4.
\end{aligned} \tag{3.8}$$

To compute the above two-fold integrals, we can apply the quadrature rule two times on the support areas respectively. The specific support areas for each of the outer integrals need be chosen respectively. For I_1, the support area of outer integral is Ω_s; for I_2, it is the support area of the basis function $\phi_j(\mathbf{x})$; for I_3, it is the support area of basis function $\phi_i(\mathbf{x})$; for I_4, it is the intersection region between the support areas of $\phi_i(\mathbf{x})$ and $\phi_j(\mathbf{x})$. The support area of each inner integral is the intersection region between $B(\tilde{\mathbf{x}},\delta(\tilde{\mathbf{x}}))$ ($\tilde{\mathbf{x}}$ is the quadrature point taken in the corresponding outer integral) and the support of basis function. Note that the integrals on the dual horizon $\widetilde{B}(\mathbf{x},\delta(\mathbf{y}))$ vanish in (3.7). In other words, in the finite element discretization for the proposed dual-horizon nonlocal diffusion model, we only need to compute the integrals over the traditional sphere horizon $B(\mathbf{x},\delta(\mathbf{x}))$. The quadratures over the intersection region of the sphere horizons and the mesh elements would be much easier and more accurate.

Except the finite element method, there also exist quite a few other numerical methods for solving the nonlocal diffusion models including the mesh-free method, the

quadrature-based finite difference method and the collocation method and they are all based on the strong form (consisting of single-fold integrals) of the target model. For the nonlocal diffusion equations with constant horizon, these methods would be preferred because of its low computation cost compared to the finite element method based on double-fold integrals. On the other hand, if we apply these methods to solve the dual-horizon nonlocal diffusion models, the integral over the intersection area between the dual-horizons and the mesh elements in (2.11) need to be computed. However the geometry of the dual horizon $\widetilde{B}(\mathbf{x}, \delta(\mathbf{y}))$ could be highly irregular as shown in Fig. 1 (right), and so are the intersection regions between the dual-horizons and the mesh elements. Thus the integrals for the intersection area between the dual-horizons and the mesh elements would be very hard to accurately compute and easily induce large quadrature errors. This could get even worse when it comes to the regions where the horizon parameter function $\delta(\mathbf{x})$ varies very quickly.

4. Numerical experiments

In this section, we use the piecewise linear finite element ($p = 1$) and carry out several numerical experiments for the dual horizon nonlocal diffusion model (2.7) in two and three dimensions ($n = 2, 3$) to illustrate the usage of the variable horizon and demonstrate the effectiveness of the finite element discretization. In all examples, the nonlocal kernel functions $\kappa(\mathbf{x}, \mathbf{y})$ is chosen to be the form of (2.3) with $s = 1$, which is a common choice in many existing nonlocal diffusion models. For simplicity, the diffusion coefficient is taken to be a constant $a(\mathbf{x}) \equiv 1$. The numerical solutions are expected to converge to the exact solution of the nonlocal problem with at best second order as $h \to 0$.

Example 4.1. In this example the two-dimensional domain Ω_s is taken to be $\Omega_s = (-1, 1) \times (-1, 1)$. We regard the spatially dependent horizon parameter $\delta(\mathbf{x})$ as a material parameter and set it to

$$\delta(x_1, x_2) = \begin{cases} 0.2, & \text{if} \quad x_1 < -0.1, \\ 0.15 - 0.5x_1, & \text{if} \quad -0.1 \le x_1 < 0.1, \\ 0.1, & \text{if} \quad x_1 \ge 0.1, \end{cases} \tag{4.1}$$

then the nonlocal volume constrained boundary Ω_c is determined accordingly. We choose the smooth exact solution as $u(x_1, x_2) = x_1^3 + x_2^2$. The boundary condition $g(x_1, x_2)$ in (2.7) are then calculated directly by the exact solution, and the source term $f(x_1, x_2)$ is obtained by applying a highly accurate Gaussian quadrature to approximate the left-hand side of (2.7) at each point.

As is shown in Fig. 2, the domain Ω_s in this example can be divided into three subdomains according to the horizon function $\delta(\mathbf{x})$. In the left subdomain the horizon parameter $\delta(\mathbf{x}) = 0.2$, in the right one the horizon $\delta(\mathbf{x}) = 0.1$ and in the middle one the horizon parameter $\delta(\mathbf{x}) = 0.15 - 0.5x_1$ which serves as the transition region. The

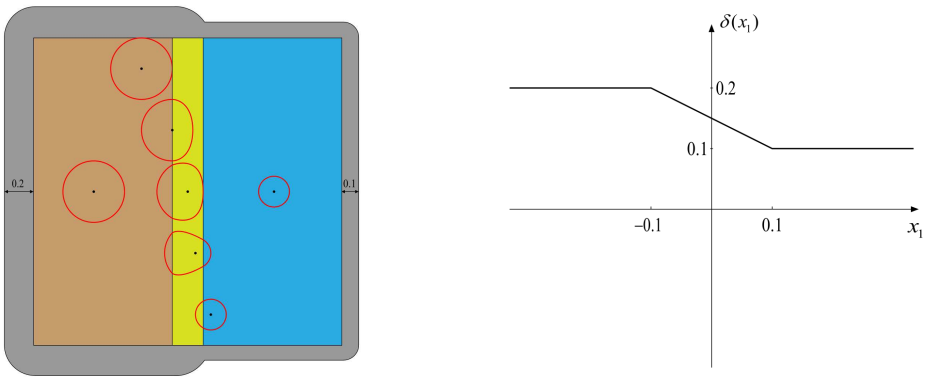

Figure 2: Illustration of the computational domain and the dual horizons $\widetilde{B}(\mathbf{x}, \delta(\mathbf{y}))$ at some typical points (left) and the horizon parameter function (right) for Example 4.1, where Ω_s consists of the brown, yellow and brown regions and Ω_c is the gray region.

geometry of the dual horizon $\widetilde{B}(\mathbf{x}, \delta(\mathbf{y}))$ at some typical points is also illustrated in Fig. 2. For points away from the transition subdomain, i.e. $x_1 < -0.3$ and $x_1 > 0.2$, the dual influence area $\widetilde{B}(\mathbf{x}, \delta(y))$ is a standard disk, however for the points near the transition area $-0.3 \leq x_1 \leq 0.2$, the dual influence area turns to be an irregular geometry, which varies with x_1. It is obvious that the intersection areas between these dual horizons and the mesh elements are irregular, which would lead to more serious quadrature errors. A set of uniform rectangular meshes for the domain $(-1, 1) \times (-1, 1)$ are generated with $N = 10, 20, 40, 80, 160$ respectively, and the piecewise bilinear basis functions are used for the finite element discretization. Numerical results on the solution errors measured by the L^∞ and L^2 norms are reported in Table 1. The L^2 errors show approximately second order convergence as expected. For exceedingly small δ, the convergence orders are slightly below the optimal value 2, which might be caused by the inexact calculations of the integrals in the numerical implementation.

Table 1: Numerical results on the solution errors and corresponding convergence rates by the piecewise bilinear finite element discretization in Example 4.1.

h	$\|e^h\|_\infty$	CR	$\|e^h\|_2$	CR
1/10	9.1323e-02	-	2.3474e-02	-
1/20	2.7876e-02	1.81	5.6415e-03	2.04
1/40	9.8771e-03	1.68	1.5464e-03	1.91
1/80	3.3778e-03	1.71	4.7208e-04	1.81
1/160	1.2112e-03	1.67	1.6144e-04	1.71

Example 4.2. In this example, we investigate the so-called δ-convergence of the proposed finite element discretization, a typical case of the asymptotic compatibility test, that is, as both the horizon parameter $\delta(\mathbf{x})$ and the grid size h go to zero at a fixed ratio, the approximate solution of the nonlocal problem (2.7) converges to that of

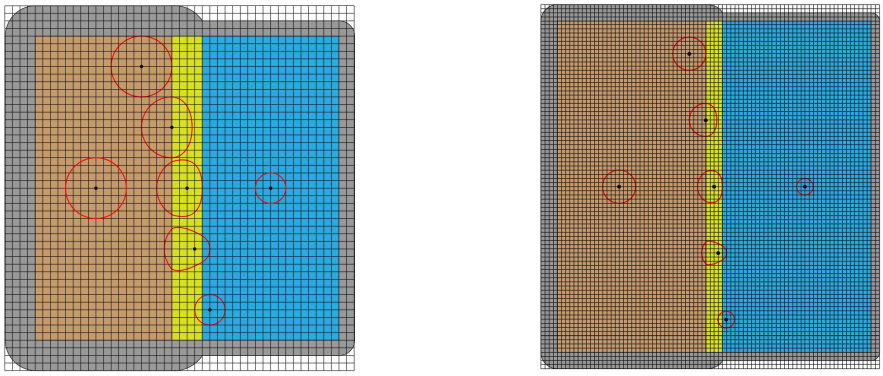

Figure 3: Illustration of the computational domain and the dual horizons $\widetilde{B}(\mathbf{x},\delta(\mathbf{y}))$ at some typical points under two levels of uniform meshes for Example 4.2. Note here that the ratio $\delta(\mathbf{x})/h$ is fixed for all levels of meshes.

the corresponding classical local diffusion problem (2.9). We take the domain $\Omega_s = (-1,1)\times(-1,1)$ and the exact solution $u(x_1,x_2) = x_1^3x_2^3$, and set the horizon function $\delta(\mathbf{x})$ as

$$\delta(x_1,x_2) = \begin{cases} 4h, & \text{if} \quad x_1 < -2h, \\ 3h - 0.5x_1, & \text{if} \quad -2h \le x_1 < 2h, \\ 2h, & \text{if} \quad x_1 \ge 2h. \end{cases} \tag{4.2}$$

The source term f, the volume constrained boundary Ω_c and the boundary condition g are again determined accordingly.

The set of uniform rectangular meshes with $N = 10, 20, 40, 80, 160$ respectively and the piecewise bilinear basis functions are again used for the finite element discretization. Similar to the case in Example 4.1, the domain Ω_s can be divided into three subdomains. As shown in Fig. 3, in the left subdomain the ratio between the horizon parameter and the mesh size is fixed to be $\delta(\mathbf{x})/h = 4$, in the right one $\delta(\mathbf{x})/h = 2$, and in the middle transition one $\delta(\mathbf{x})/h = 3 - 0.5x_1/h$. Table 2 reports numerical results on the compatibility errors measured by the L^∞ and L^2 norms and the corresponding convergence rates. It is observed that the numerical solution does converge to the local

Table 2: Numerical results on the solution compatibility errors and corresponding convergence rates by the piecewise bilinear finite element discretization with the fixed $\delta(x)/h$ ratio in Example 4.2.

h	$\|e^h\|_\infty$	CR	$\|e^h\|_2$	CR
1/10	8.8765e-02	-	3.1259e-02	-
1/20	2.8333-02	1.77	1.0325e-02	1.74
1/40	8.8431e-03	1.79	3.1522e-03	1.81
1/80	3.4116e-03	1.61	1.1303e-03	1.67
1/160	1.4693e-03	1.54	3.7771e-04	1.73

solution along the mesh refinement (as well as the decreasing of $\delta(\mathbf{x})$) with a order between 1.67 and 1.74 in L^2 norm and between 1.54 and 1.77 in L^∞ norm.

Example 4.3. In the last example, we extend the above numerical experiments to three dimensions. The domain Ω_s is taken to be $\Omega_s = (-1,1)\times(-1,1)\times(-1,1)$. As done in Example 4.1, we divide the domain into three parts along the x_1 axis, the left one with $\delta(\mathbf{x}) = 0.2$, the right one with $\delta(\mathbf{x}) = 0.1$ and a transition region with $\delta(\mathbf{x}) = 0.15 - 0.5x_1$. The exact solution is taken to be $u(x_1,x_2,x_3) = x_1^2x_2^2x_3^2$. The source f, the volume constrained boundary Ω_c and the boundary condition g are determined accordingly.

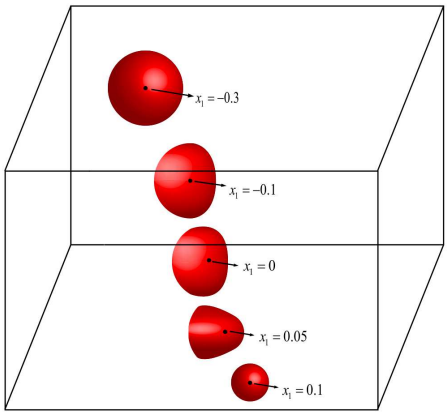

Figure 4: Illustration of the computation domain and the dual horizons $\widetilde{B}(\mathbf{x},\delta(\mathbf{y}))$ at some typical points for Example 4.3.

As shown in Fig. 4, the dual horizon $\widetilde{B}(\mathbf{x},\delta(\mathbf{y}))$ varies from left to right along the x_1 axis, that is, the ball with radius $\delta(\mathbf{x}) = 0.2$ gradually changes to a smaller ball with radius $\delta(\mathbf{x}) = 0.1$ and in between they are irregular balls. We use the piecewise trilinear basis functions for the finite element discretization to solve the dual-horizon nonlocal diffusion equation. We take the uniform meshes with $N = 10, 20, 40, 80$ respectively. Numerical results on the solution errors measured by the L^∞ and L^2 norms and corresponding convergence rates are reported in Table 3. We observe that the convergence orders are around $5/3$, again somehow below the optimal value 2.

Table 3: Numerical results on the solution errors and corresponding convergence rates by the piecewise trilinear finite element discretization in Example 4.3.

h	$\|e^h\|_\infty$	CR	$\|e^h\|_2$	CR
1/10	1.1323e-02	-	8.3474e-03	-
1/20	3.6973e-03	1.75	3.1036e-03	1.64
1/40	1.4088e-03	1.62	5.2288e-03	1.71
1/80	5.1123e-03	1.66	2.0883e-03	1.61

5. Conclusions

This paper presents and analyzes a dual-horizon nonlocal diffusion model and its finite element discretization. In particular, an irregular influence area, named as the dual-horizon, is included in this nonlocal model. The dual-horizon is naturally induced by the action-reaction law, which guarantees the mass conservation for nonlocal diffusion models under variable horizon parameter. However, the geometry of dual horizon could be highly irregular and so is the intersection area between the dual horizon and the mesh elements. If we apply numerical discretizations directly to the original strong form of the proposed model, such as quadrature-based finite difference methods, the mesh-free method or the collocation method, the integrals over these intersection areas need to be accurately evaluated, which are often very hard in practice. By noticing that the dual-horizon term vanishes in the corresponding variational form of the model, we develop a finite element discretization for its numerical solution, which can avoid these numerical quadrature difficulties.

Acknowledgments

H. Tian's work is partially supported by the National Natural Science Foundation of China (Grants 11801533, 11871454), Fundamental Research Funds for the Central Universities (Grant 202042008) and Natural Science Foundation of Shandong Province (Grant ZR2019ba031).

References

[1] F. Bobaru and M. Duangpanya, *A peridynamic formulation for transient heat conduction in bodies with evolving discontinuities*, J. Comput. Phys. 231 (2012), 2764–2785.

[2] F. Bobaru, M. Yang, L.F. Alves, S.A. Silling, E. Askari, and J. Xu, *Convergence, adaptive refinement, and scaling in 1D peridynamics*, Int. J. Numer. Meth. Eng. 77 (2009), 852–877.

[3] E. Buades, B. Coll, and J. M. Morel, *Image denoising methods. A new nonlocal principles*, SIAM Rev. 52 (2010), 113–147.

[4] X. Chen and M. Gunzburger, *Continuous and discontinuous finite element methods for a peridynamics model of mechanics*, Comput. Methods Appl. Mech. Engrg. 200 (2011), 1237–1250.

[5] M. D'Elia, Q. Du, M. Gunzburger, and R. Lehoucq, *Finite range jump processes and volume-constrained diffusion problems*, Technical Report #SAND 2014-2584J, Sandia National Laboratories, Albuquerque, 2014.

[6] M. D'Elia, M. Perego, P. Bochev, and D. Littlewood, *A coupling strategy for nonlocal and local diffusion models with mixed volume constraints and boundary conditions*, Comput. Math. Appl. 71 (2016), 2218–2230.

[7] M. D'Elia, X. Tian, and Y. Yu, *A physically consistent, flexible, and efficient strategy to convert local boundary conditions into nonlocal volume constraints*, SIAM J. Sci. Comput. 42 (2020), 1935–1949.

[8] Q. Du, M. Gunzburger, R. Lehoucq, and K. Zhou, *Analysis and approximation of nonlocal diffusion problems with volume constraints*, SIAM Rev. 54 (2012), 667–696.
[9] Q. Du, M. Gunzburger, R. Lehoucq, and K Zhou, *A nonlocal vector calculus, nonlocal volume-constrained problems, and nonlocal balance laws*, Math. Models Methods Appl. Sci. 23 (2013), 493–540.
[10] Q. Du and Z. Huang, *Numerical solution of a scalar one-dimensional monotonicity-preserving nonlocal nonlinear conservation law*, J. Math. Res. Appl. 37 (2017), 1–18.
[11] Q. Du, Z. Huang, and R. Lehoucq, *Nonlocal convection-diffusion volume-constrained problems and jump processes*, Dis. Cont. Dyn. Sys. B 19 (2014), 373–389.
[12] Q. Du, L. Ju, X. Li, and Z. Qiao, *Stabilized linear semi-implicit schemes for the nonlocal Cahn-Hilliard equation*, J. Comput. Phys. 363 (2018), 39–54.
[13] Q. Du, L. Ju, L. Tian, and K Zhou, *A posteriori error analysis of finite element method for linear nonlocal diffusion and peridynamic models*, Math. Comp. 82 (2013), 1889–1922.
[14] Q. Du, J. Kamm, R. Lehoucq, and M. Parks, *A new approach for a nonlocal nonlinear conservation law*, SIAM J. Appl. Math. 72 (2012), 464–487.
[15] Q. Du, X. Li, and L. Ju, *Maximum principle preserving exponential time differencing schemes for the nonlocal Allen-Cahn equation*, SIAM J. Num. Anal. 57 (2019), 875–898.
[16] Q. Du, Y. Tao, and X. Tian, *Nonlocal diffusion and peridynamic models with Neumann type constraints and their numerical approximations*, Appl. Math. Comp. 305 (2017), 282–298.
[17] Q. Du, Y. Tao, X. Tian, and J. Yang, *Robust a posteriori stress analysis for approximations of nonlocal models via nonlocal gradients*, Comp. Methods Applied Mech. and Engrg. 310 (2016), 605–627.
[18] Q. Du, Y. Tao, X. Tian, and J. Yang, *Asymptotically compatible discretization of multi-dimensional nonlocal diffusion models and nonlocal Green's function*, IMA J. Numer. Anal. 39 (2019), 607–625.
[19] Q. Du, L. Tian, and X. Zhao, *A convergent adaptive finite element algorithm for nonlocal diffusion and peridynamic models*, SIAM J. Numer. Anal. 51 (2013), 1211–1234.
[20] Q. Du and J. Yang, *Fast and accurate implementation of Fourier spectral approximations of nonlocal diffusion operators and its applications*, J. Comput. Phys. 332 (2017), 118–134.
[21] G. Gilboa and S. Osher, *Nonlocal linear image regularization and supervised segmentation*, Multiscale Model. Simul. 6 (2007), 595–630.
[22] G. Gilboa and S. Osher, *Nonlocal operators with applications to image processing*, Multiscale Model. Simul. 7 (2008), 1005–1028.
[23] M. Gunzburger and R. B. Lehoucq, *A nonlocal vector calculus with application to nonlocal boundary value problems*, Multiscale Model. Simul. 8 (2010), 1581–1598.
[24] W. Hu, Y. Ha, and F. Bobaru, *Peridynamic model for dynamic fracture in unidirectional fiber-reinforced composites*, Comput. Methods Appl. Mech. Engrg. 220 (2012), 247–261.
[25] R. Lipton, *Cohesive dynamics and brittle fracture*, J. Elasticity 124 (2016), 143–191.
[26] R. Macek and S. Silling, *Peridynamics via finite element analysis*, Finite Elem. Anal. Des. 43 (2007), 1169–1178.
[27] E. Oterkus, E. Madednci, and A. Agwai, *Peridynamic thermal diffusion*, J .Comput. Phys. 265 (2014), 71–96.
[28] E. Oterkus, E. Madednci, and S. Ote, *Peridynamic shell membrane formulation*, Procedia Struct. Integr. 28 (2020), 411–417.
[29] E. Oterkus, B. Wang, and S. Ote, *Effect of horizon shape in peridynamics*, Procedia Struct. Integr. 28 (2020), 418–429.
[30] K. Painter, J. M. Bloomfield, J. Sherratt, and A. Gerisch, *A nonlocal model for*

contact attraction and repulsion in heterogeneous cell populations, Bull. Math. Biol. 77 (2015), 1132–1165.

[31] H. REN, X. ZHUANG, AND T. RABCZUK, *Dual-horizon peridynamics: A stable solution to varying horizons*, Comput. Methods Appl. Mech. Engrg. 318 (2017), 0–20.

[32] P. SELESON, M. GUNZBURGER, AND M. L. PARKS, *Interface problems in nonlocal diffusion and sharp transitions between local and nonlocal domains*, Comput. Methods Appl. Mech. Engrg. 266 (2013), 185–204.

[33] S. SILLING, *Reformulation of elasticity theory for discontinuities and long-range forces*, J. Mech. Phys. Solids 48 (2000), 175–209.

[34] S. SILLING, M. EPTON, O. WECKNER, J. XU, AND E. ASKARI, *Peridynamic states and constitutive modeling*, J. Elast. 88 (2007), 151–184.

[35] S. SILLING AND R LEHOUCQ, *Peridynamic theory of solid mechanics*, Adv. Appl. Mech. 44 (2010), 73–168.

[36] S. SILLING, M ZIMMERMANN, AND R. ABEYARATNE, *Deformation of a peridynamic bar*, J. Elast. 73 (2003), 173–190.

[37] Y. TAO, X. TIAN, AND Q. DU, *Nonlocal models with heterogeneous localization and their application to seamless local-nonlocal coupling*, Multi. Model Simul 17(3) (2019), 1051–1075.

[38] X. TIAN AND Q. DU, *Analysis and comparison of different approximation to nonlocal diffusion and linear peridynamic equations*, SIAM J. Numer. Anal. 51 (2013), 3458–3482.

[39] X. TIAN AND Q. DU, *Asymptotically compatible schemes and applications to robust discretization of nonlocal models*, SIAM J. Numer. Anal. 52 (2014), 1641–1665.

[40] X. TIAN AND Q. DU, *Trace theorems for some nonlocal function spaces with heterogeneous localization*, SIAM J. Math. Anal. 49 (2017), 1621–1644.

[41] H. TIAN, L. JU, AND Q. DU, *Nonlocal convection-diffusion problems and finite element approximations*, Comput. Methods Appl. Mech. Engrg. 289 (2015), 60–78.

[42] H. TIAN, L. JU, AND Q. DU, *A conservative nonlocal convection-diffusion problems and asymptotically compatible finite difference discretization*, Comput. Methods Appl. Mech. Engrg. 320 (2017), 46–67.

[43] H. TIAN, J. ZHANG, AND L. JU, *A spectral collocation method for nonlocal diffusion equations with volume constrained boundary conditions*, Appl. Math. Comput. 370 (2019), 875–895.

[44] H. WANG, E. OTERKUS, AND S. OTE, *Peridynamic modelling of fracture in marine lithium-ion batteries*, Ocean Eng. Oceanogr. 151 (2018), 257–267.

[45] H. WANG AND H. TIAN, *A fast and faithful collocation method with efficient matrix assembly for a two-dimensional nonlocal diffusion model*, Comput. Methods Appl. Mech. Engrg. 273 (2014), 19–36.

[46] C. ZHENG, Q. DU, X. MA, AND J. ZHANG, *Stability and error analysis for a second-order fast approximation of the local and nonlocal diffusion equations on the real line*, SIAM J. Numer. Anal. 58 (2020), 1893–1917.

[47] K. ZHOU AND Q. DU, *Mathematical and numerical analysis of linear peridynamic models with nonlocal boundary condition*, SIAM J. Numer. Anal. 48 (2010), 1759–1780.